

Dream

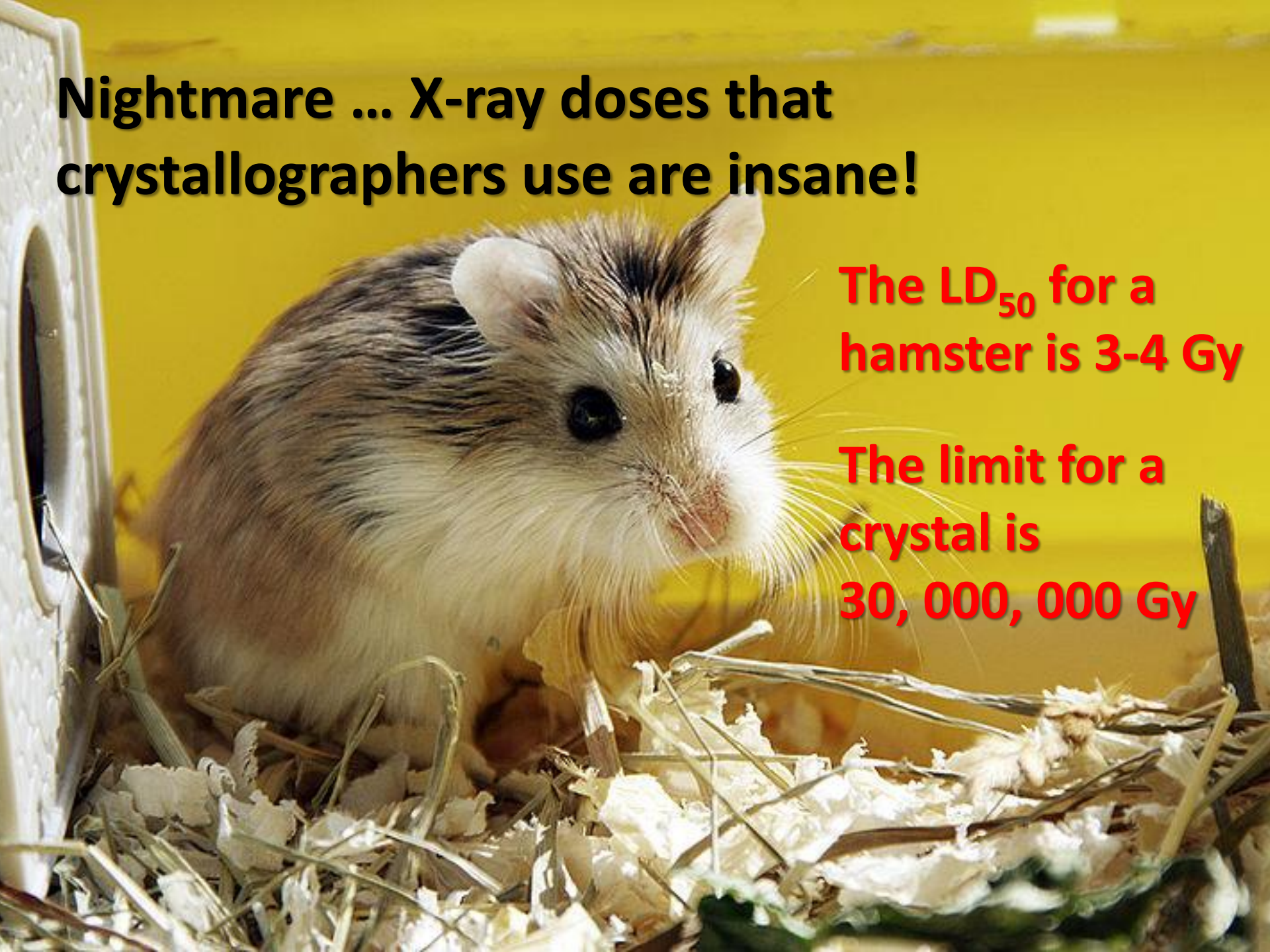


If we knew both mechanism and rates could we produce a model for radiation damage that explained the known damage and perhaps allowed extrapolation to an undamaged state?

**Nightmare ... X-ray doses that
crystallographers use are insane!**

**The LD₅₀ for a
hamster is 3-4 Gy**

**The limit for a
crystal is
30, 000, 000 Gy**



So how do we avoid the nightmare
and keep the dream?

A radiation damage model for crystallographers requires multiple pathways

- Swarts et al. (2007) studied the dose dependence of radiation products from DNA crystals by in situ X-ray irradiation and Electron Paramagnetic Resonance (EPR).
- EPR measures unpaired electrons and therefore free radical formation (it quantifies free radical production).
- This study showed a transition in the dose rate response at 10–100 kGy - A single one-to-one correspondence between radical intermediate and end product can not explain this result.
- In typical X-ray diffraction data collection, a single image is recorded at a dose on the orders of kGy.

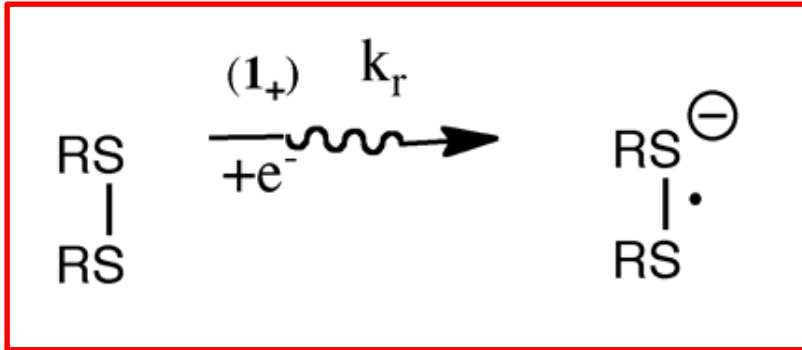
What is a multiple pathway?

- At incident X-ray energies associated with macromolecular crystallography the photoelectric effect dominates.
- This creates a fast electron along with an associated cation.
- The photoelectron propagates along a track creating additional energetic electrons and cations.
- The ejected electrons eventually thermalize primarily creating anions.
- The resulting track is a branched inhomogeneous distribution of anions, cations, and excitations.
- As the dose rate increases, the probability of on track overlapping with another increases, any model has to take into account these multiple pathways.

Simplify: Consider only the disulphide bond

- The original model based upon the DNA research is expanded.
- The hypothesis is that a S-S bond in macromolecular crystals would not be cleaved as a result of a single one-electron reduction but by a one electron reduction followed by protonation then a second one-electron reduction.
- Concurrence of these events while possible within a single track of ionizing radiation has a much higher probability when tracks overlap (as dose rate increases).

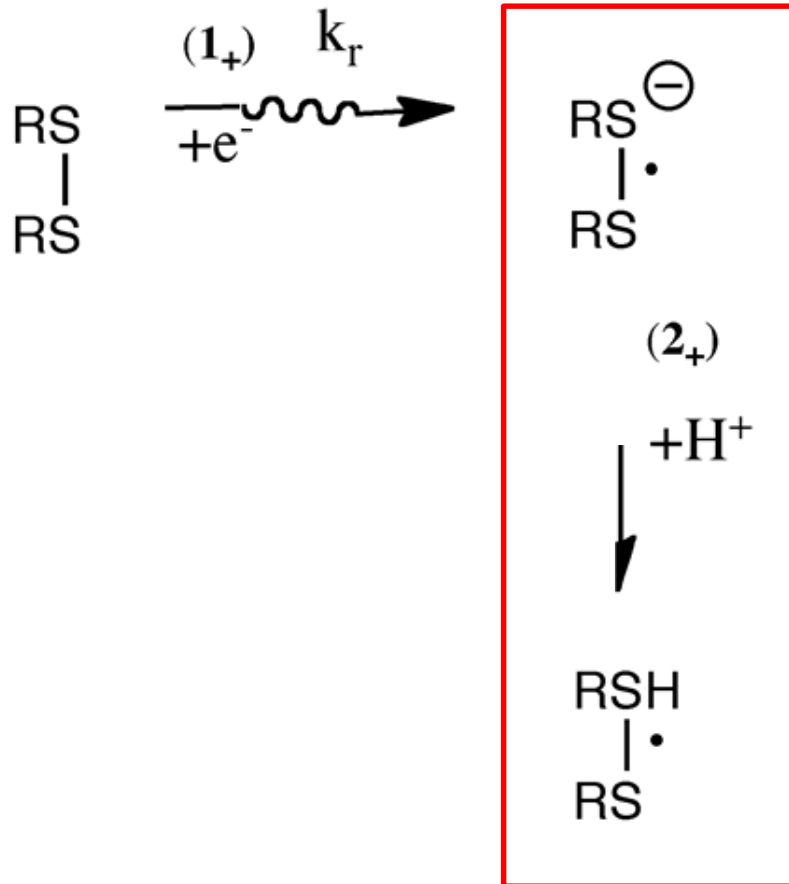
A model for disulfide damage



Step 1₊: A free radical electron yields the radical anion RSSR^{•-} with the rate constant k_r

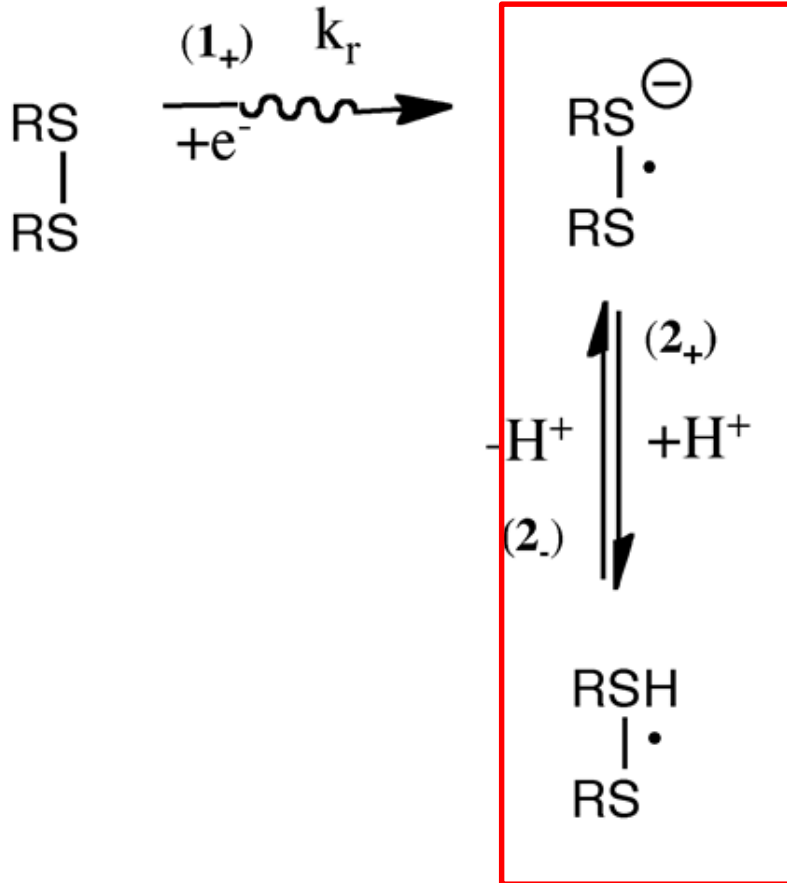
Developed by Bill Bernhard

A model for disulfide damage



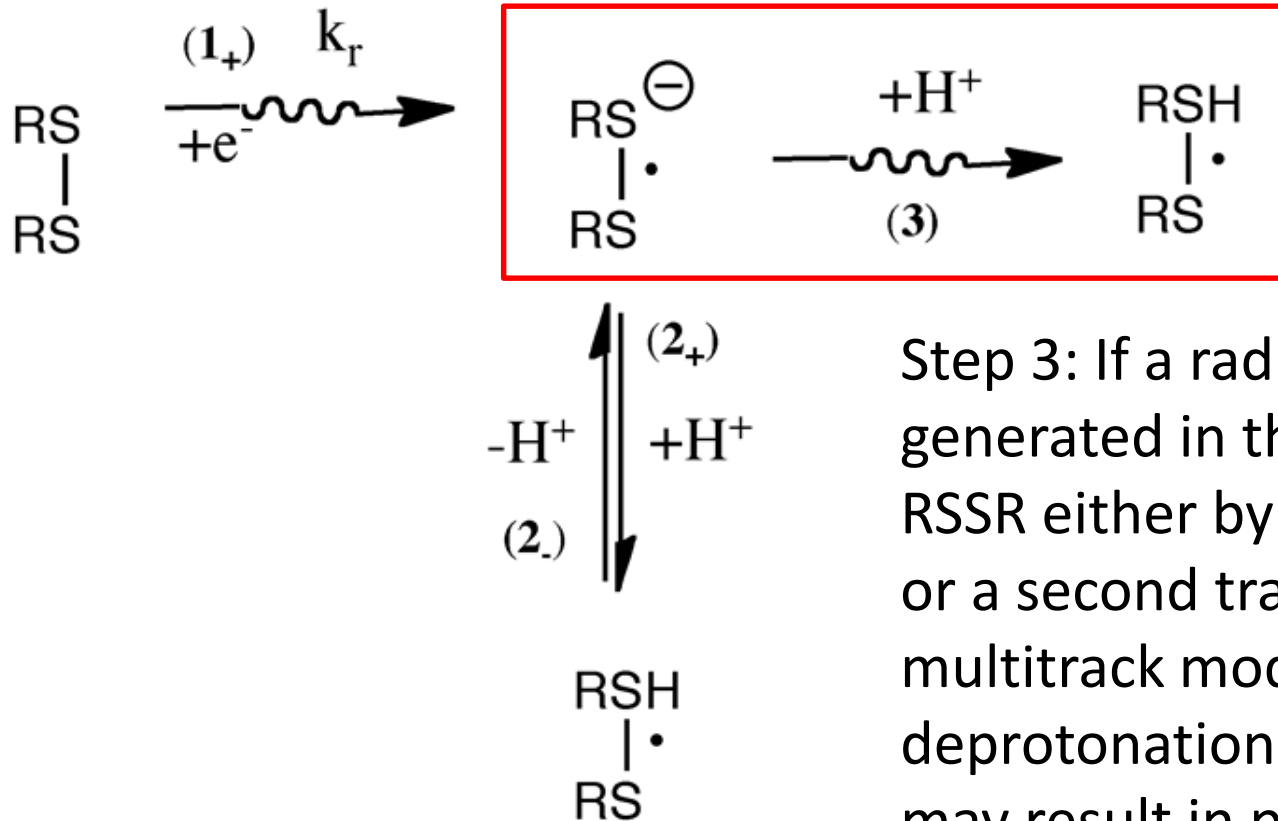
Step 2₊: If RSSR is coordinated with a favorable proton donor then proton transfer gives the neutral radical SSH•

A model for disulfide damage



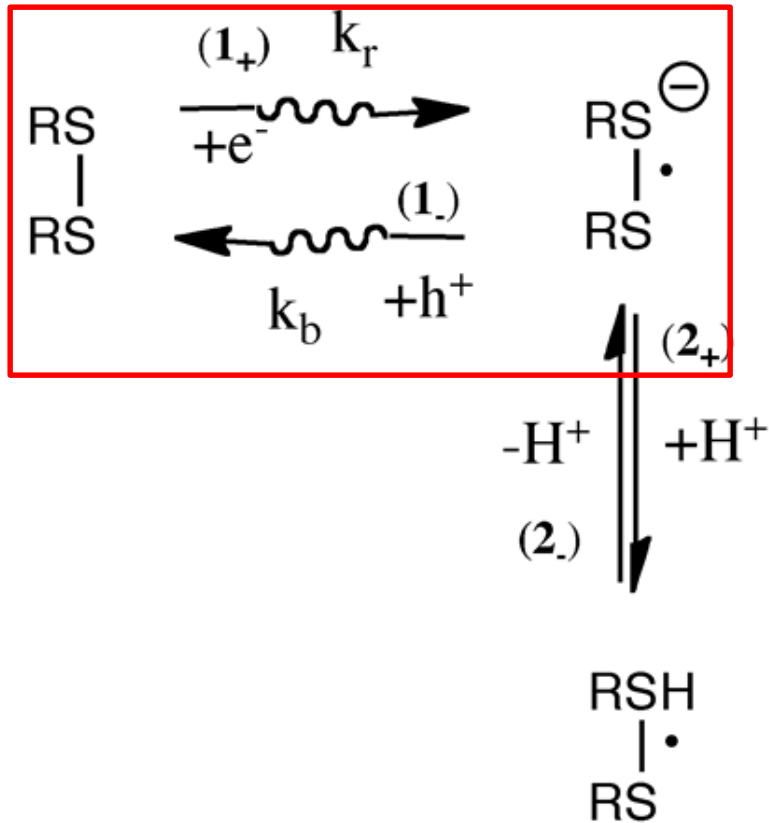
Step 2_.: The reaction is reversible with the back reaction providing a repair pathway.

A model for disulfide damage



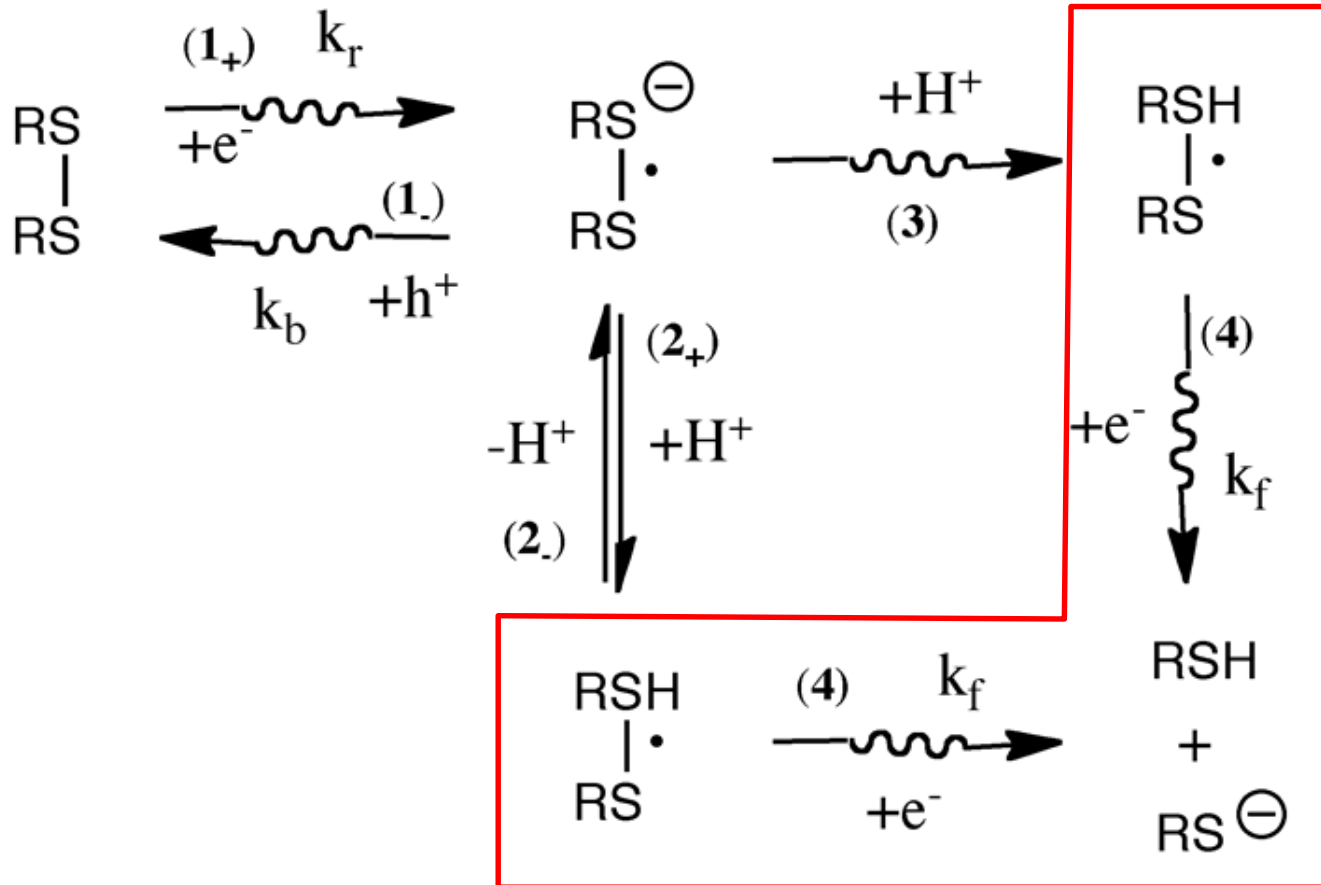
Step 3: If a radical cation is generated in the proximity of RSSR either by the same track or a second track (the multitrack model) deprotonation of this radical may result in protonation of SS^\ominus to become RSS(H)^\cdot . This is non-reversible.

A model for disulfide damage



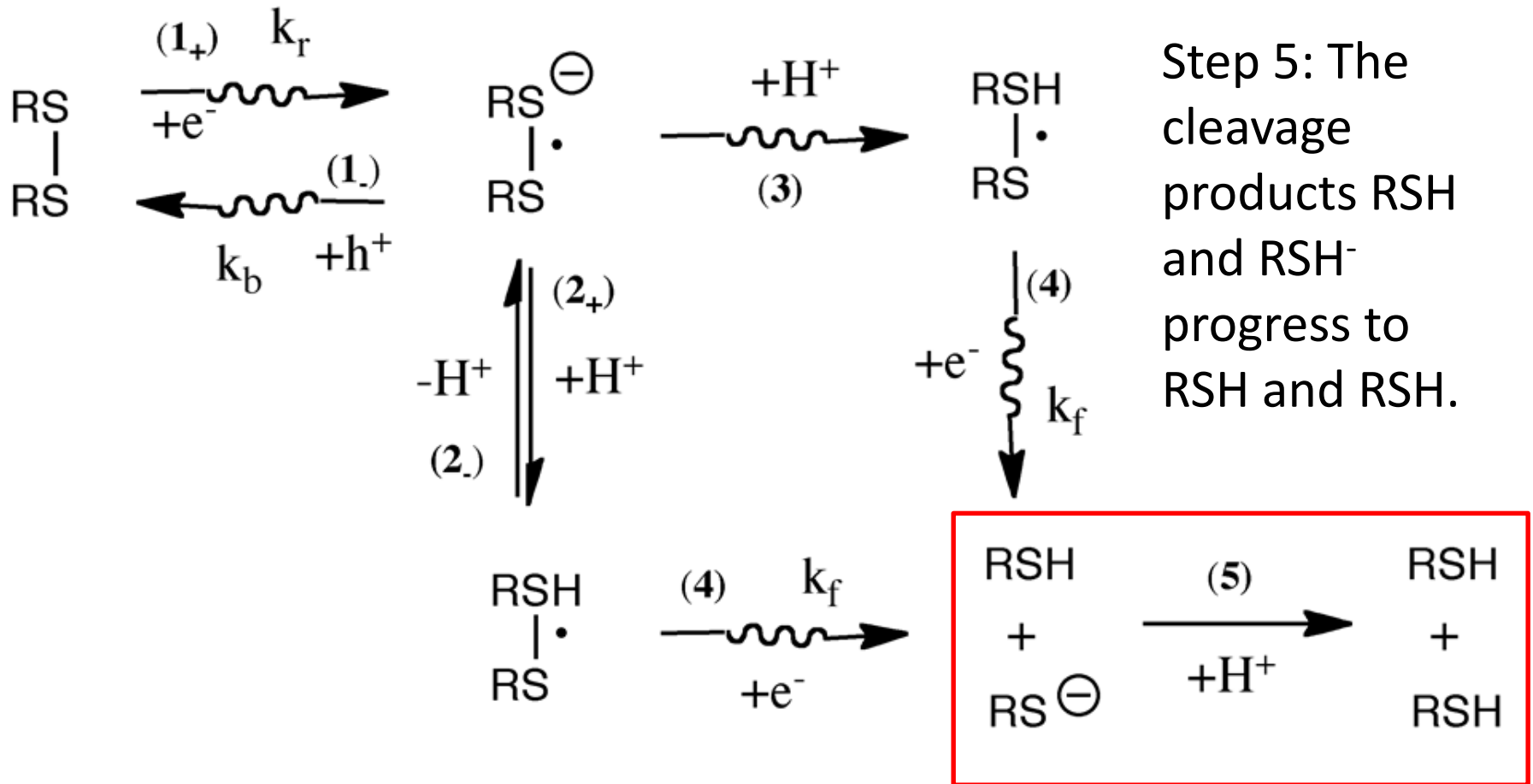
Step 1-: The $\text{SS}^{\bullet-}$ radicals will be highly reactive with holes (radical cations designated h^+) and electrons generated by overlapping tracks yielding a repair pathway with a rate constant k_b .

A model for disulfide damage

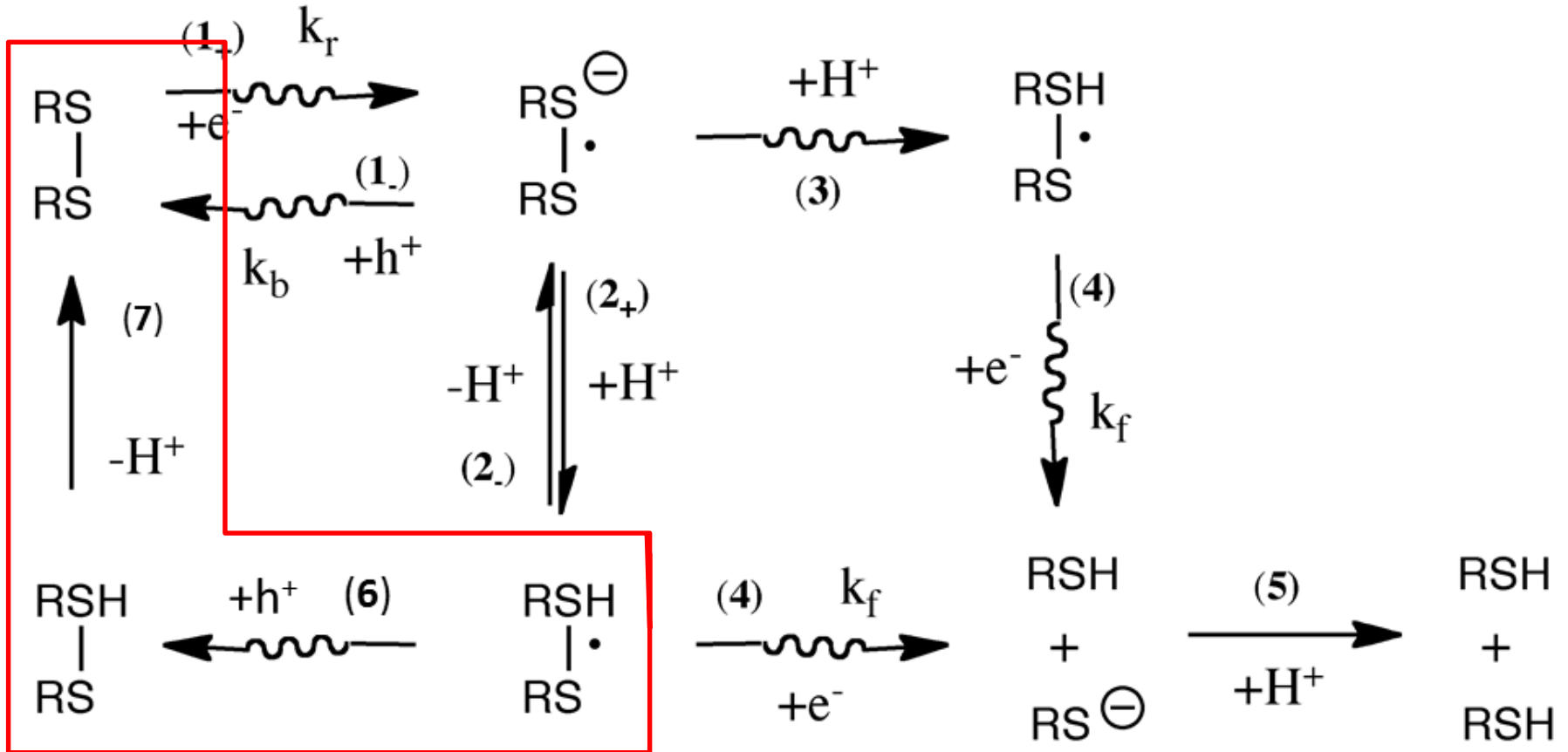


Step 4: Electron attachment drives $\text{SS}(\text{H})^\bullet$ forward to the product with a rate constant k_f .

A model for disulfide damage

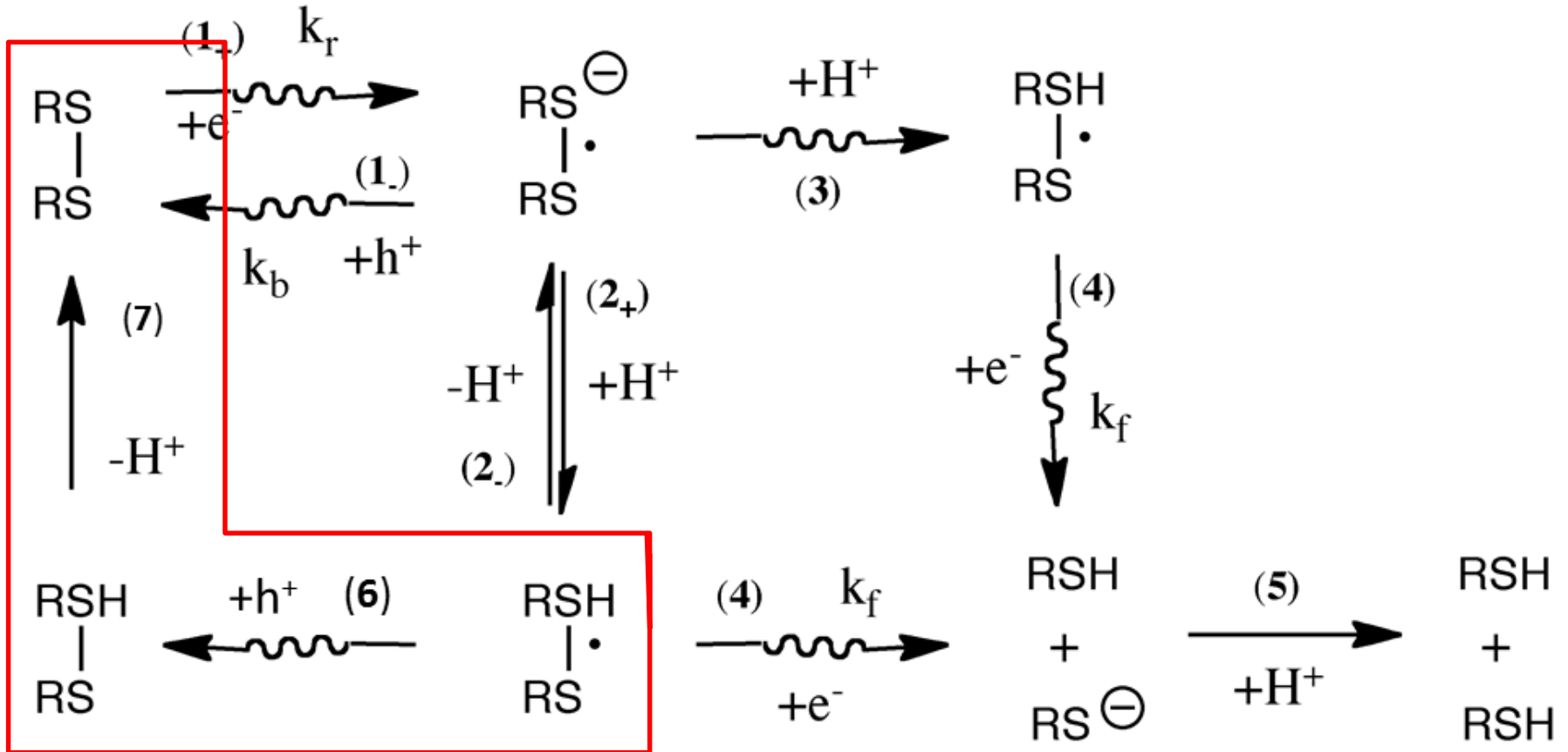


A model for disulfide damage



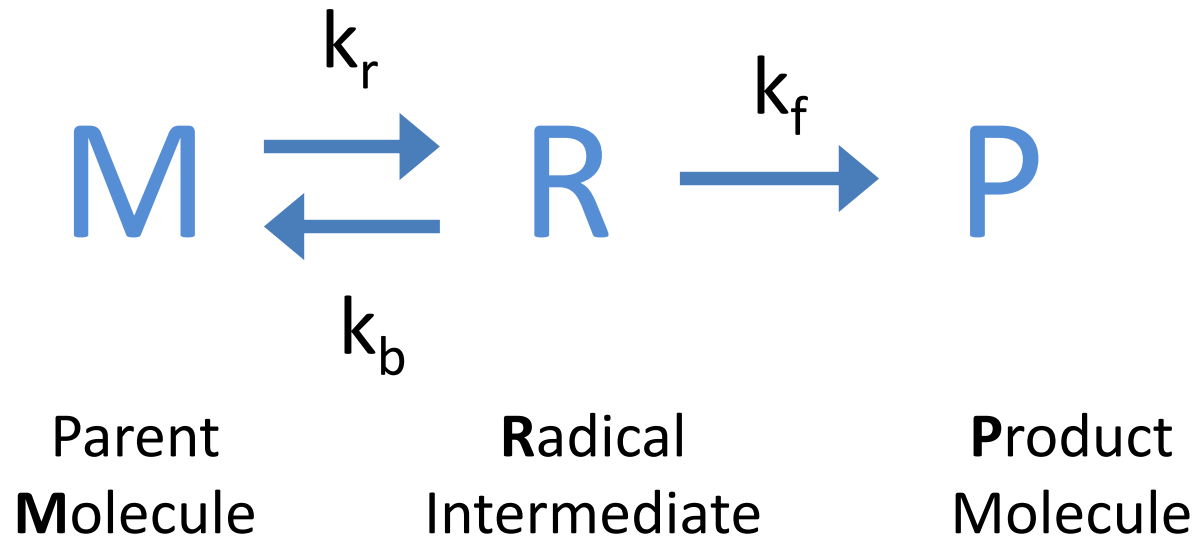
Step 6 and 7: Protonated radical repair pathway

A model for disulfide damage



Step 6 and 7: Protonated radical repair pathway

A proposed mathematical description



This can be modeled as two first order reactions, the first being radiation driving a reversible reaction between a parent molecule M and a radical intermediate R and in the second radiation irreversibly driving the radical R to product P.

Details are provided in Sutton et al., Acta Cryst D69, 2381-2394 (2013)

How do we test this?

- Study the process with atomic detail:
 - X-ray crystallography (shows the electron density and loss or gain of electrons)
- Quantitate the chemistry going on
 - Electron Paramagnetic Resonance (measures unpaired electrons, distinct spectrum for different species) with *in situ* irradiation
- Link the two measurements (at very different doses) with UV/visible microspectrophotometry

Use a model protein with disulphide bonds

- Chicken Egg White Lysozyme - not hen :)
- The model itself is based on physical-chemical properties and therefore its application is not limited to any single protein.

Experimental detail

- X-ray data were collected at SSRL with an X-ray energy of 12 keV (1.033 Å) and the beam was attenuated by 93.6% giving a flux of 3.8×10^{10} phs⁻¹.
- Each data set starting at the same position as the first ensuring that the same area of the crystal was irradiated during each dataset.
- The crystal was approximately 0.3 x 0.3 x 0.3 mm with the beam (approximating a top hat profile) illuminating an area of 0.2 x 0.2 mm.

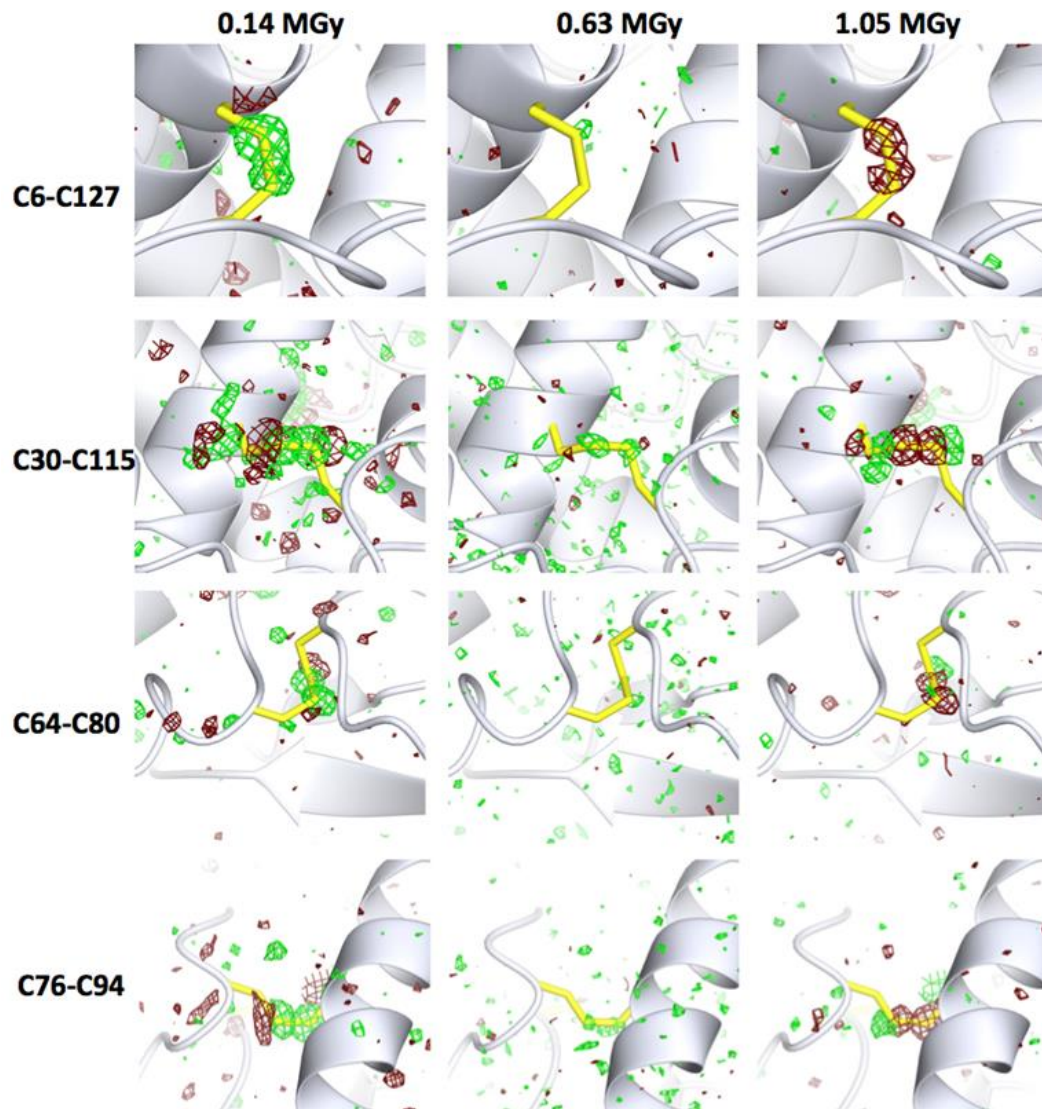
Experimental detail

- A total of 15 datasets over 57° were collected using a 2 s exposure and oscillation angle of 1° , each data set starting at the same position as the first ensuring that the same area of the crystal was irradiated during each dataset.
- The crystal was approximately $0.3 \times 0.3 \times 0.3$ mm with the beam (approximating a top hat profile) illuminating an area of 0.2×0.2 mm.
- The absorbed dose was estimated using the program RADDOSE, but not adjusted for fresh regions of the crystal that rotated into the beam (estimated to reduce the calculated absorbed dose by less than 0.2% per $^\circ$).

Absorbed dose

Data sets	15
Absorbed dose per data set	0.07 MGy
Total dose	1.05 MGy

Disulphide bonds



Isomorphous difference density maps $Fo_n - Fo_1$ (where n is the data set number) around the four disulfide bonds present in lysozyme.

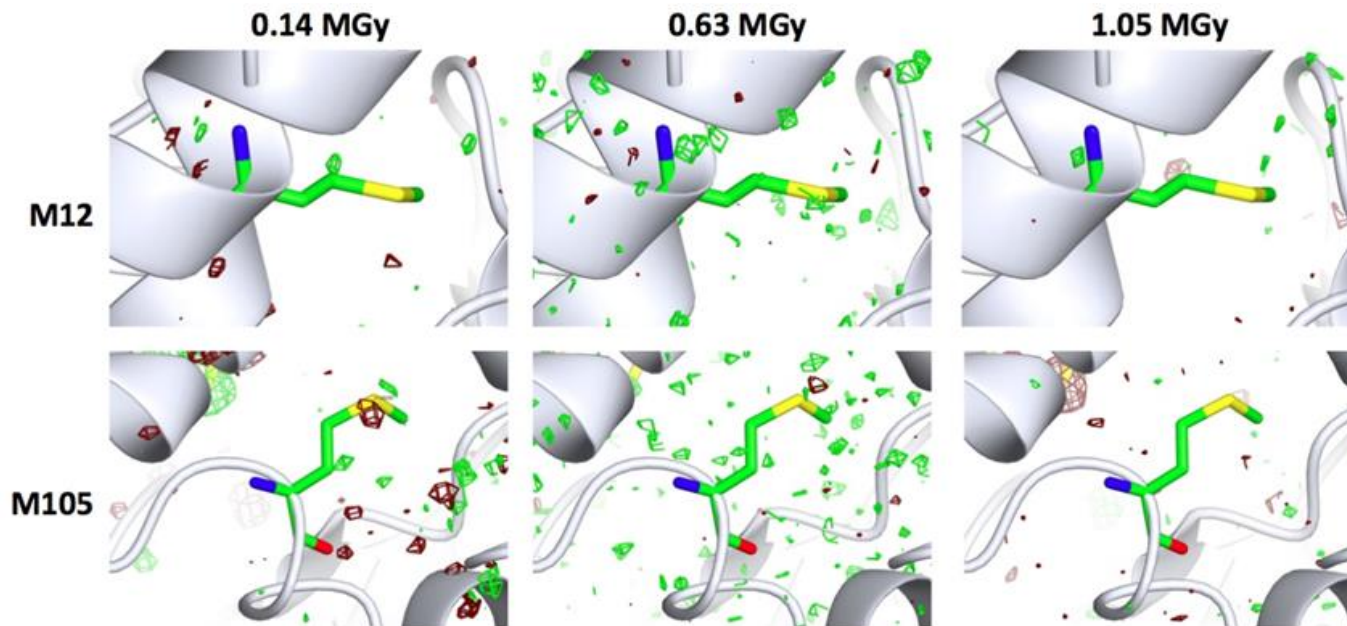
Maps are shown for $Fo_2 - Fo_1$ (0.14 MGy), $Fo_9 - Fo_1$ (0.63 MGy) and $Fo_{15} - Fo_1$ (1.05 MGy).

Disulfide bonds are highlighted in yellow.

Maps are contoured at $+3\sigma$ (green) and -3σ (red).

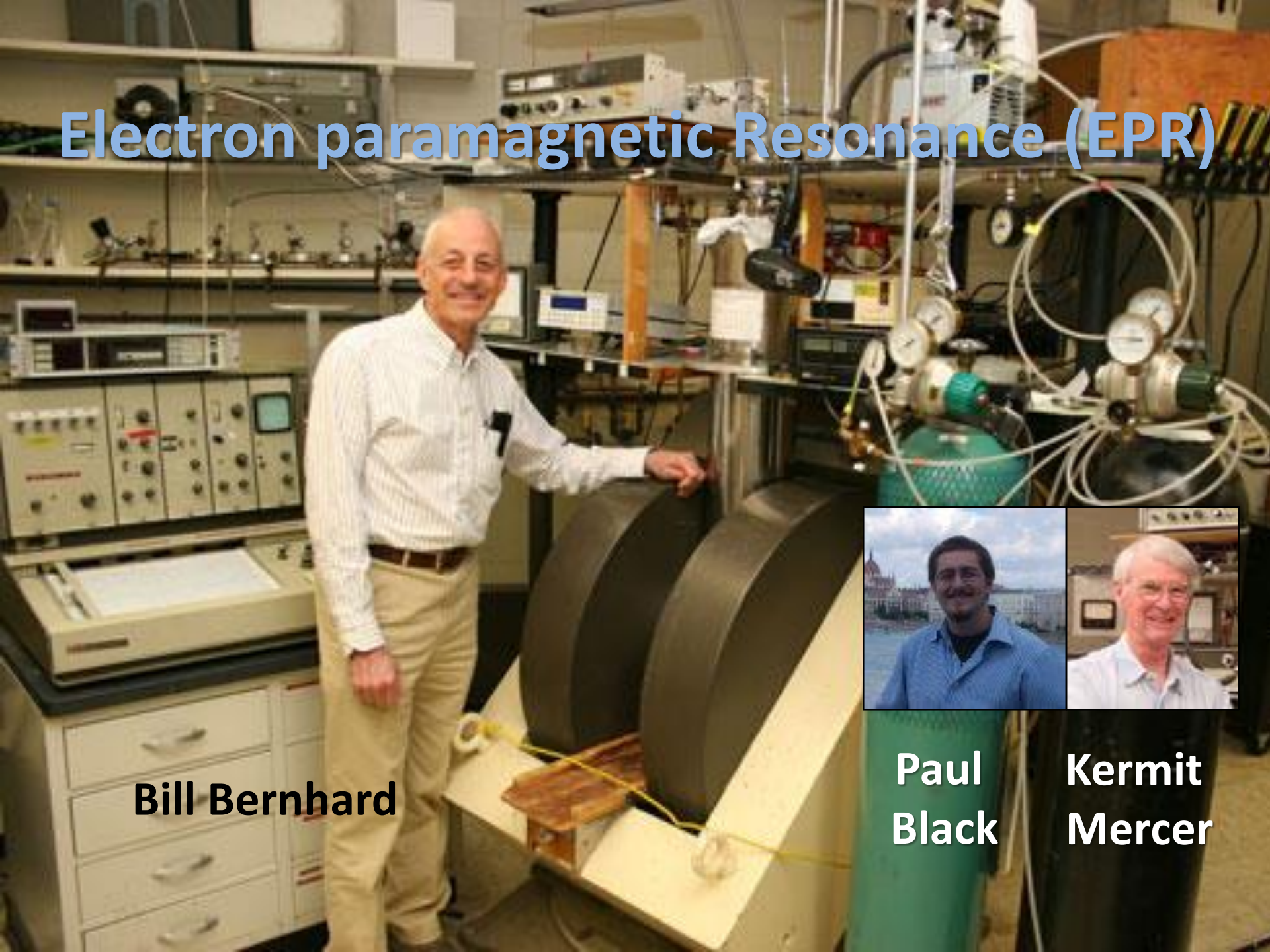
For C6-C127 the top most part of the bond is C6 with the bottom being C127. The remaining bonds are positioned such that the label matches the residue positions in each figure with the first to the left and the second to the right. Note that the dose indicated is the cumulative dose.

Methionine residues as a control



Isomorphous difference density maps $Fo_2 - Fo_1$ (0.14 MGy) $Fo_9 - Fo_1$ (0.63 MGy) and $Fo_{15} - Fo_1$ (1.05 MGy) for residues Met12 and Met105. Maps are contoured at 3σ in green and -3σ in dark red.

Electron paramagnetic Resonance (EPR)



Bill Bernhard



**Paul
Black**



**Kermit
Mercer**

Sample tube



EPR chamber

In situ X-ray
exposure (tube
not present)



EPR Experimental Setup

- Crystals mounted in 1.0 mm outer diameter thin walled quartz glass capillaries
- Inserted one at a time into a Janis liquid helium cryostat in the EPR instrument and cooled to a temperature of 4 K in less than 30 seconds.
- No attempt was made to obtain precise information on the alignment of the crystals with respect to the magnetic field.
- Crystals were irradiated in situ with median energy 50 keV X-rays at 4 K using a Varian/Eimac OEG-76H tungsten target tube operated at 70kV, 20 mA, and filtered by a 25 μm aluminum foil.

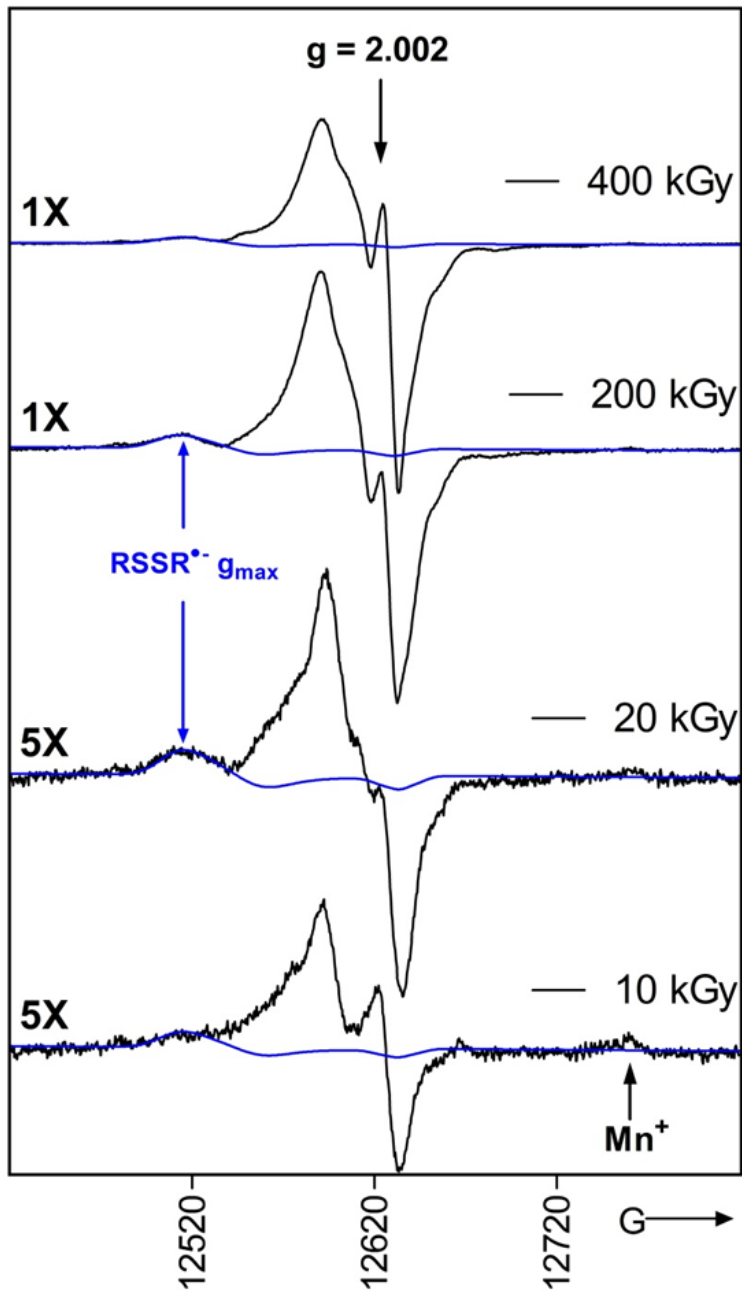
Experimental data collection

	Dimensions (mm)	Volume (mm ³) ⁺	Weight (μg)	Dose points for EPR measurements (kGy)
Crystal 1	0.60 × 0.50 x 0.40	0.12	208	5, 10, 20, 40, 60, 100, 150
Crystal 2	0.50× 0.50 x 0.25	0.06	135 [*]	10, 20, 40, 60, 100
Crystal 3	0.50× 0.50 x 0.40	0.10	185 [*]	20, 40, 100, 200, 300, 400, 500

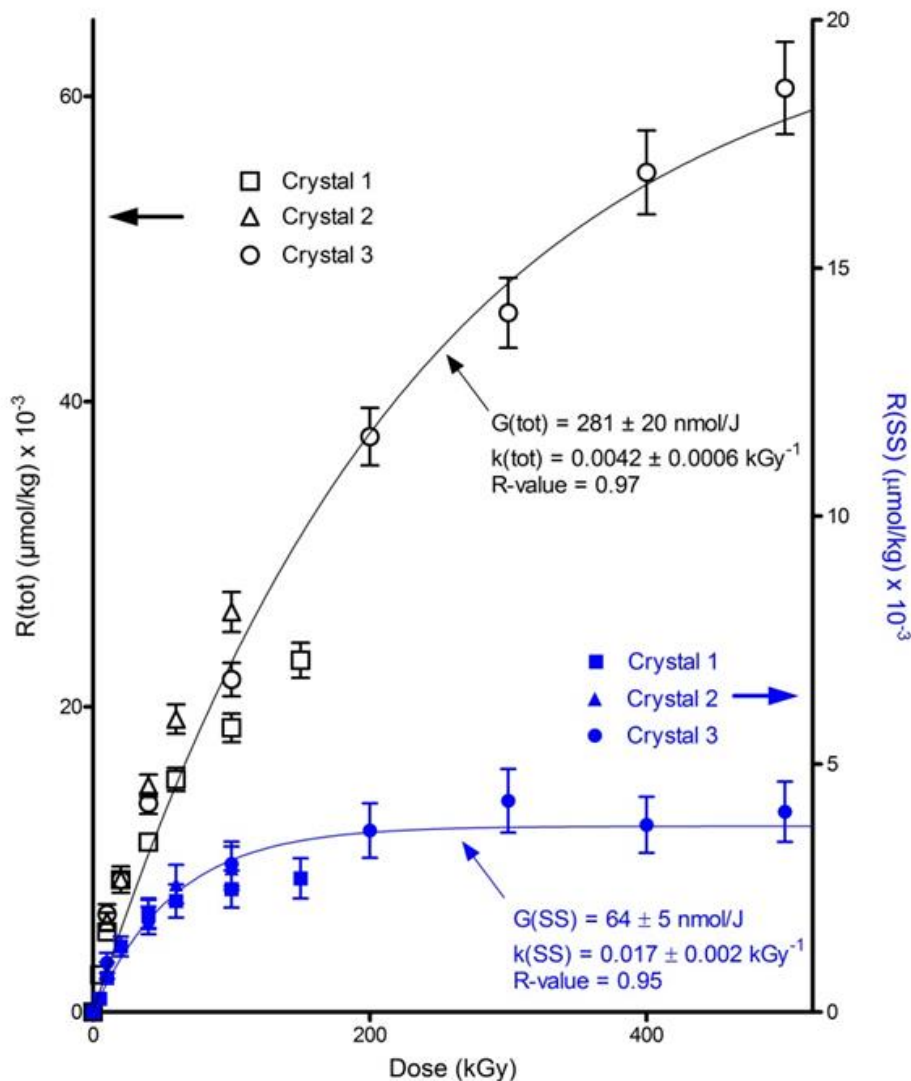
Volume is approximate, calculated by assuming a cuboid which does not take into account crystal shape. *Masses were calculated based on the measured radical yield at a dose of 20.

Crystalline ice, is not a problem

- Dose rate at the sample was $0.0125 \text{ kGy s}^{-1}$, determined by calibration with radiochromic film .
- Following irradiation, EPR data collection was performed on samples at 4 K. First-derivative EPR-absorption spectra were recorded at Q-band (35.3 GHz) microwave frequency.
- Ice irradiated at 4 K gives a distinctive 50 mT doublet. Lack of the doublet showed ice content lower than a few percent of crystal mass : the cooling procedure used created little to no water ice.
- The EPR signal is largely independent of ice type (Bednarek et al., 1998) so unlike during crystallographic studies, the type of ice formed does not impact the measurements.



- EPR spectra are shown for four different X-ray doses.
- At low doses between 10 kGy and 20 kGy, the spectrum intensity increases linearly with dose.
- At higher doses, e.g., 200 kGy to 400 kGy, a plateau is reached.
- The blue traces are simulations of the RSSH• component, is associated with the low field signal assigned exclusively to RSSH•.
- The double integral of the experimental and calculated spectra gave the radical concentrations, $R(\text{tot})$ and $R(\text{SS})$ respectively.
- The peak from the growing RSSH• component is indicated along with a peak from trace amounts of Mn^+ known to be present in the experimental setup.



The $R(\text{tot})$ data are plotted using black symbols and the $R(\text{SS})$ data are plotted using blue symbols. The curves fitting these data are derived from a non-linear least squares fit to the model.

The fitting parameters for $R(\text{tot})$ were $G(\text{tot}) = 281 \pm 20 \text{ nmolJ}^{-1}$ and $k = 4.2 \pm 0.6 \text{ MGy}^{-1}$. G is chemical yield.

For $R(\text{SS})$, the fitting parameters were calculated to be $G(\text{SS}) = 64 \pm 5 \text{ nmolJ}^{-1}$ and $k = 17 \pm 2 \text{ MGy}^{-1}$.

Saturation values for $R(\text{SS})$ vs. $R(\text{tot})$ are distinctly different, reflecting the differences in dose response properties between the radical species. $R(\text{SS})$ saturates $\sim 200 \text{ kGy}$ at a value of $R(\text{SS})_{\infty} = 3.7 \pm 0.5 \text{ mmol kg}^{-1}$, whereas $R(\text{tot})$ saturates above 500 kGy at a value of $R(\text{tot})_{\infty} = 66 \pm 10 \text{ mmol kg}^{-1}$.

Diamond Light Source



Elspeth Garman



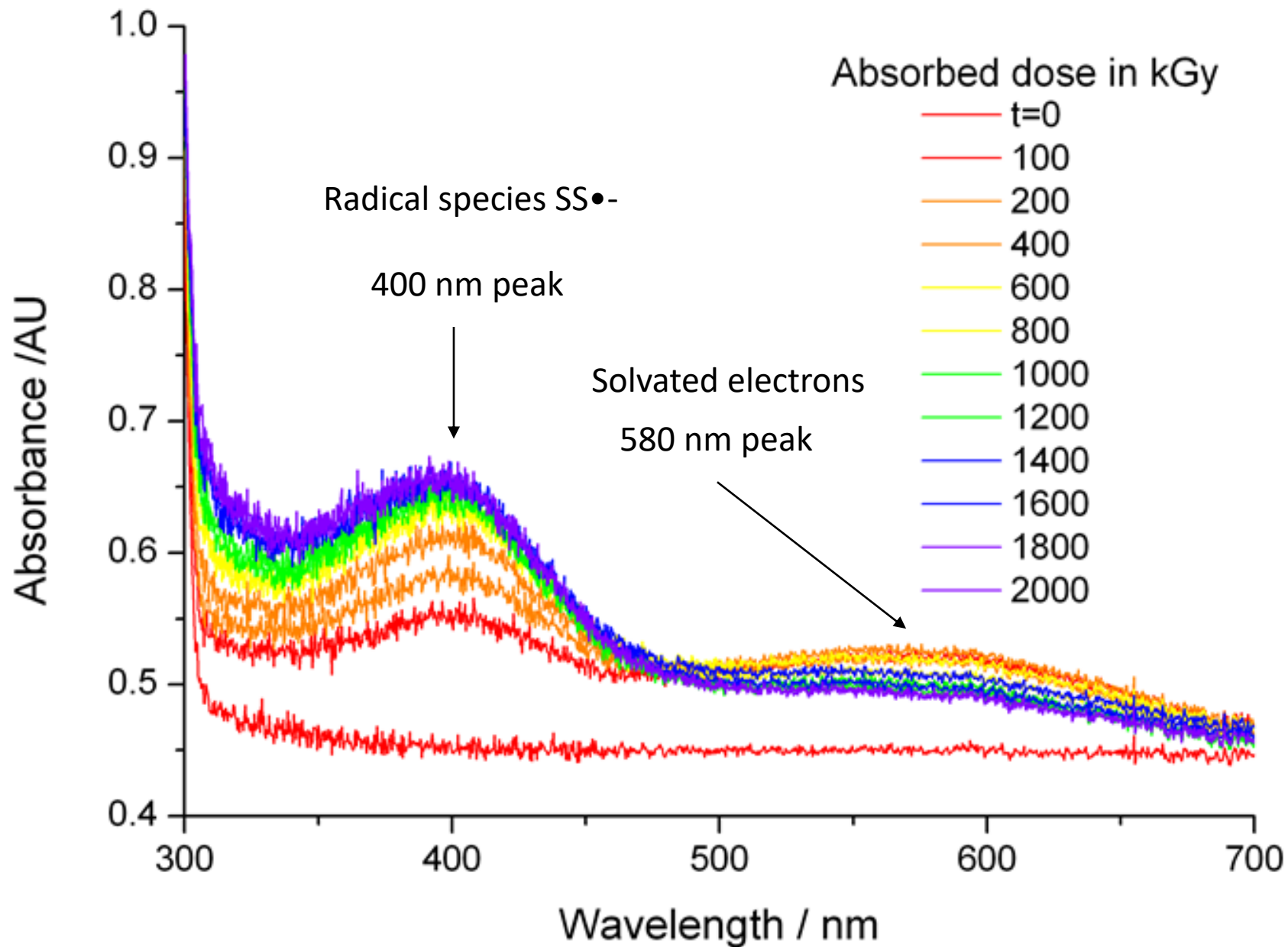
Robin Owen

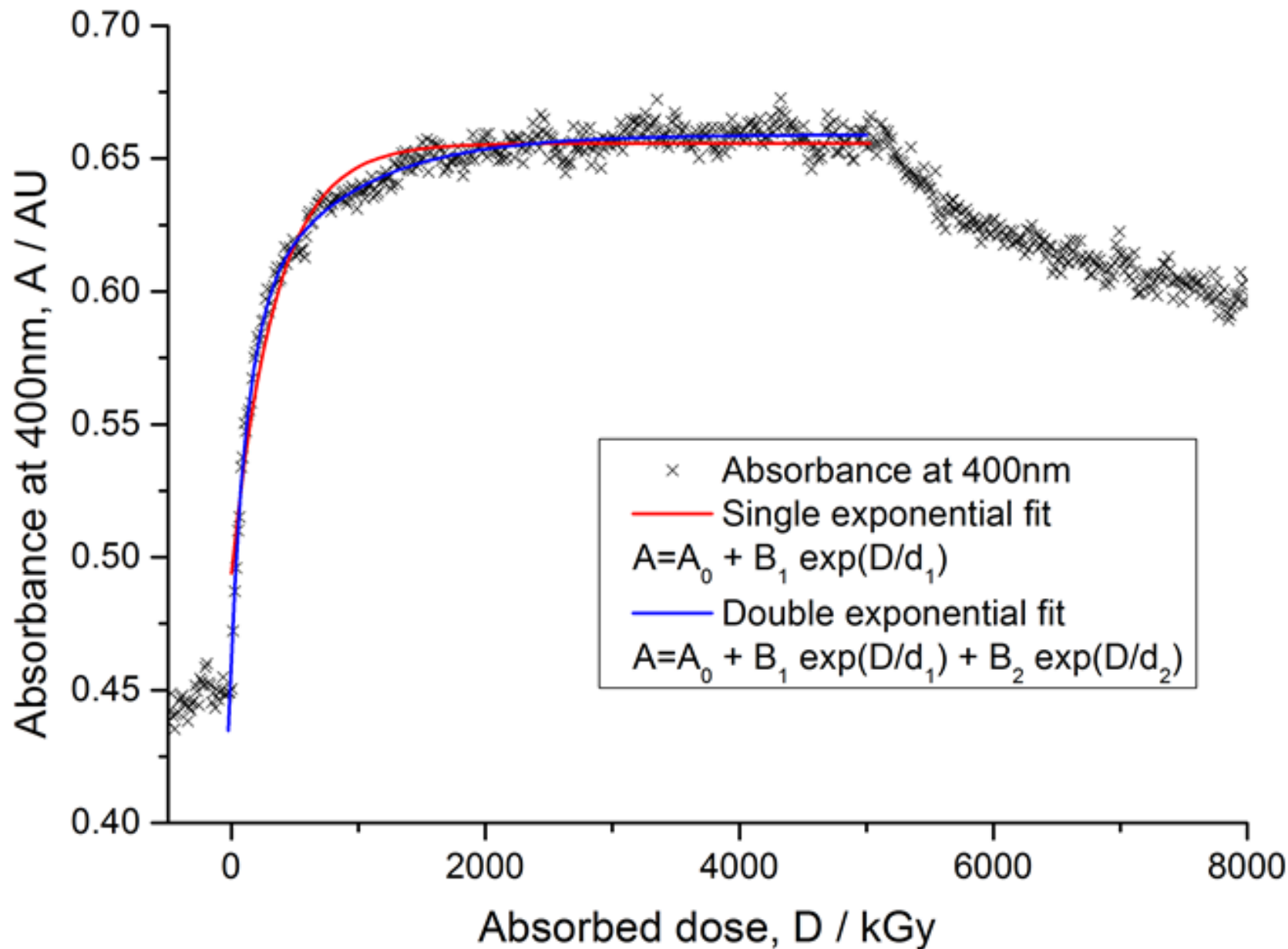
A photograph of a complex scientific instrument setup. A central black cylindrical component is mounted on a base. To its right, a robotic arm with a yellow and blue label is positioned. The setup is surrounded by various mechanical parts, cables, and a control panel on the right. The background is a metallic structure.

**Diamond
setup on I24**

UV/visible microspectrophotometry

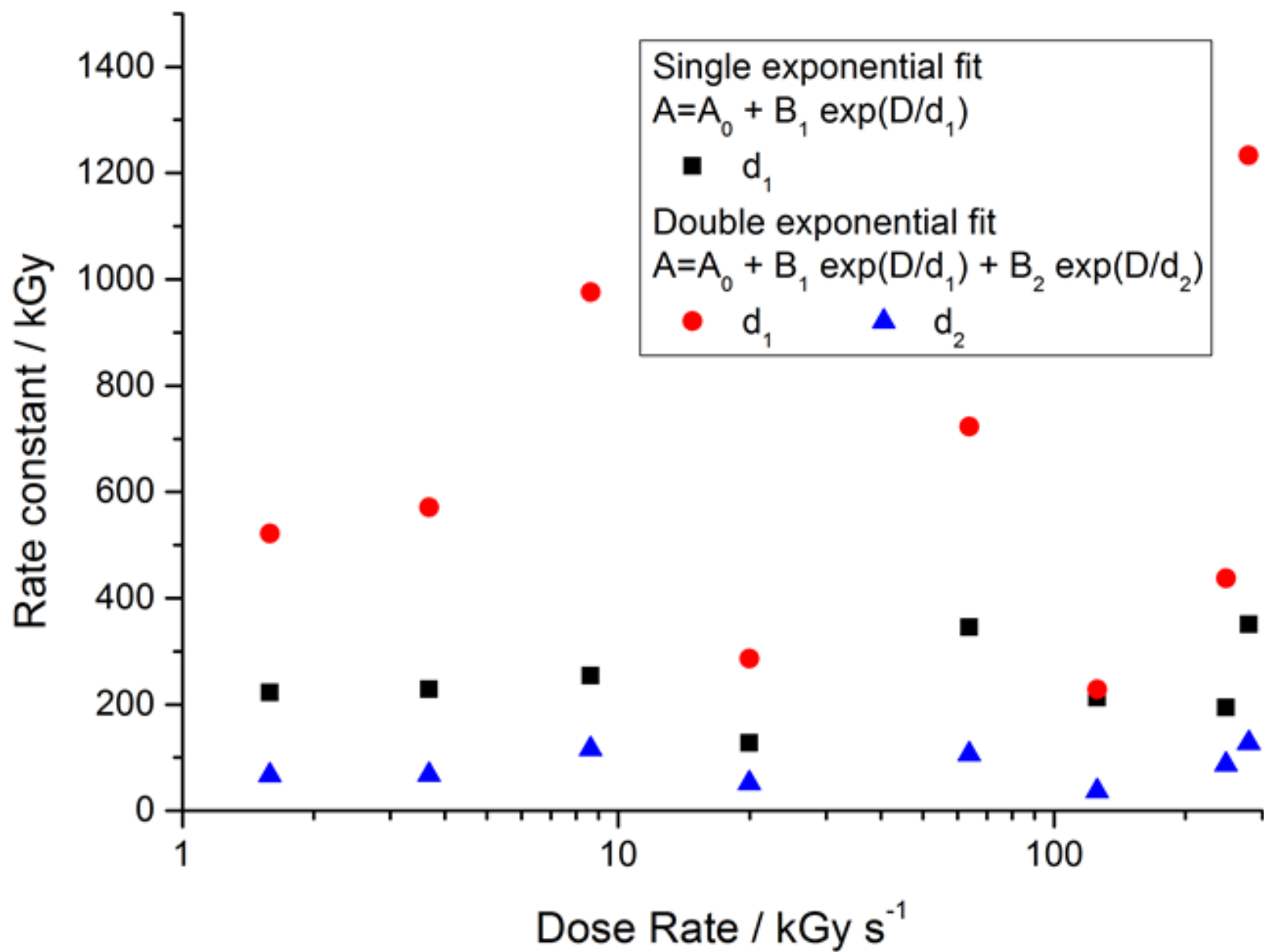
- Eight crystals were mounted in nylon loops and held at 100 K.
- They were irradiated with X-rays of energy 12.8 keV with the beam was defocused to $50 \times 50 \mu\text{m}^2$
- Incident fluxes ranging from $8.58 \times 10^9 \text{ ph s}^{-1}$ to $1.54 \times 10^{12} \text{ ph s}^{-1}$ at the sample position (filter transmission from 0.8% to 100%) - dose-rates ranging from 1.5 to 2700 kGy s^{-1} .
- Crystals were subjected to a single X-ray exposure, the duration of which varied such that the total absorbed dose was $\sim 5 \text{ MGy}$.
- Changes in UV/visible optical absorbance were measured using an in-situ microspectrophotometer with a $50 \mu\text{m}$ diameter probe beam to closely match the X-ray illuminated area.





For all 8 crystals ...

- The dose response curves were fitted to both a single and a double exponential function
- All data could be well fitted with a single or double exponential with an $R^2 \geq 0.95$, although visual inspection of fits showed that the double exponential fit better describes the data for all crystals.
- The saturating dose, D90, is defined as the point at which the absorbance reaches 90% of the maximum above baseline (where fast changes no longer dominate).

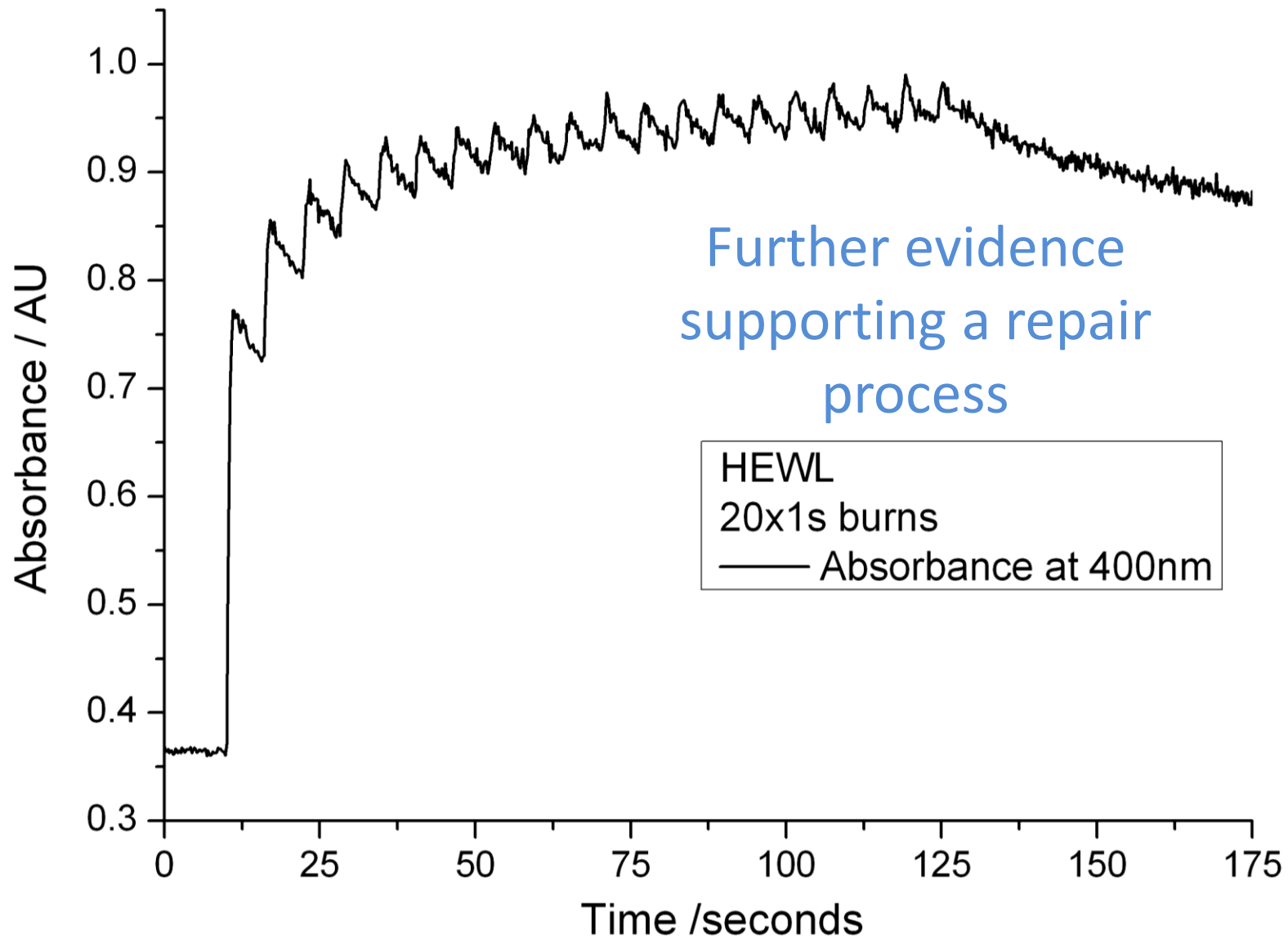


UV/visible microspectrophotometry results

- The increased absorbance at 400 nm is attributable to the radical species $SS\bullet^-$ and an increase in absorbance at this wavelength was clearly observed in all samples.
- This was accompanied by a peak in absorption at ~ 580 nm attributable to the formation of solvated electrons.
- Absorbance at 400 nm increases rapidly before saturating and the 580 nm peak due to solvated electrons has an observed maximum at the earliest recorded point.
- This peak may have been higher at earlier time points (below 200 ms) that were not captured in the experiment.

Multiple exposure with a rest period

- The change in absorbance from a series of 1 s exposures interspersed with a 5 s rest period
 - Despite a rapid reduction in absorbance when the X-ray shutter was closed for the rest period, saturation at 400 nm was still achieved rapidly with a progressively smaller change in absorption for the same additional absorbed dose.
 - The reduction in absorption seen during the rest period indicates that some fraction of $SS^{\bullet-}$ was lost due to recombination and/or protonation, but the dominating increase over time indicates that some fraction was stable



Bringing it all together

Results

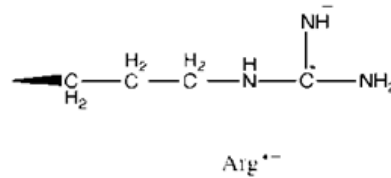
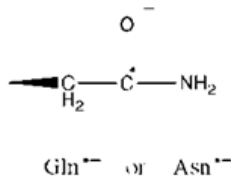
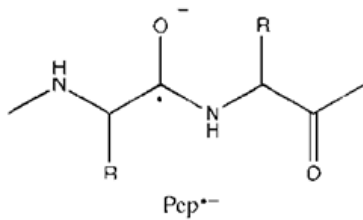
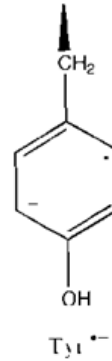
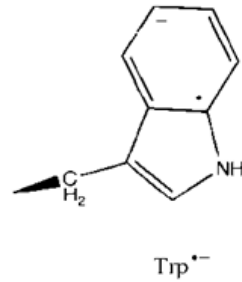
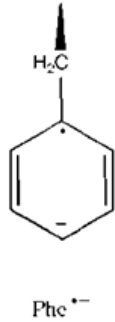
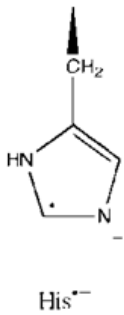
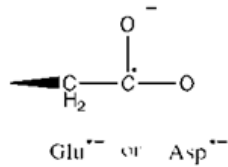
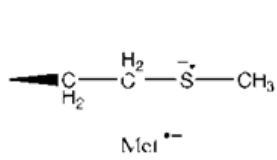
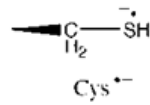
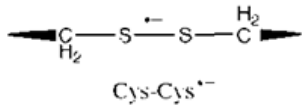
- X-ray crystallography shows radicalization of the disulphide bonds at 0.14 MGy (the lowest dose point).
- EPR shows a saturating dose of ~ 0.2 MGy
- UV/visible spectroscopy showed that disulfide radicalization appeared to saturate at an absorbed dose of approximately $\sim 0.5-0.7$ MGy (depending on the fit) at 216,000 times the dose of the EPR.
- That saturation occurs in both cases suggests that a multi-track model involving product formation due to the interaction of two separate tracks, is valid.

Results

- Our model fits well across a range of X-ray doses, explaining the data from **5 kGy** to **1.05 MGy** (EPR and crystallographic) and the microspectrophotometry data up to **~5 MGy**.
- At even the smallest absorbed dose in our range, (5 kGy), the EPR measurements indicate complete dose saturation of one-electron reduced disulfide bonds within the protein. In addition, our model predicts that the initial reduction of disulfide bridges would not result in the scission of the bond.

Even at the lowest doses used for structural investigations, disulfide bonds are already becoming radicalized.

Other amino acids ...

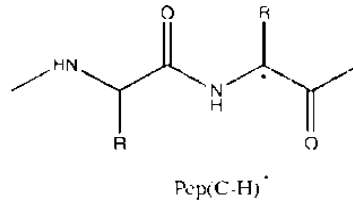
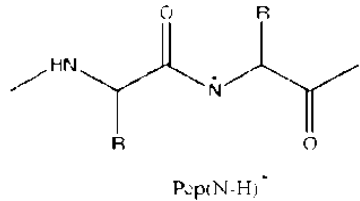
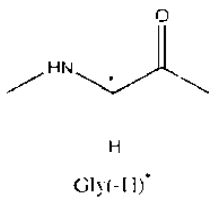
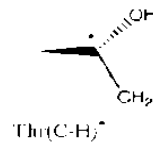
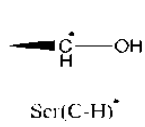
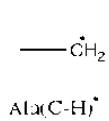
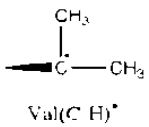
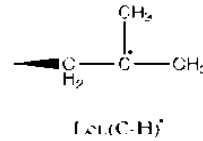
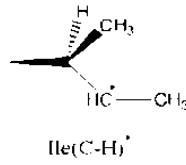
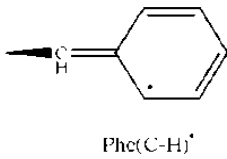
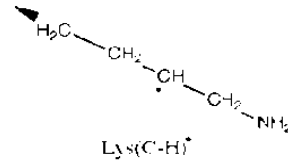
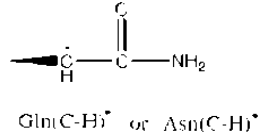
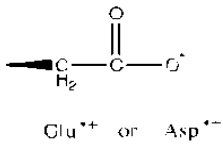
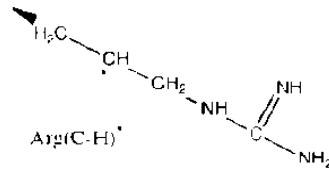
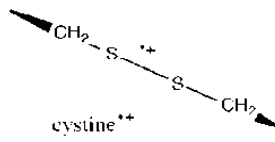
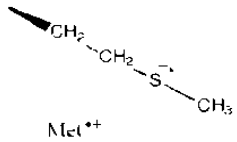
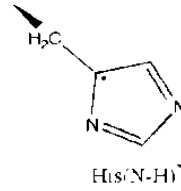
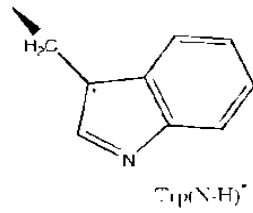
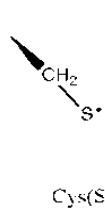
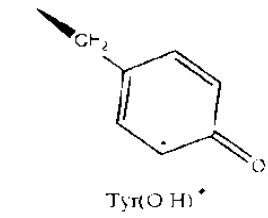


The multi-track model is not unique for disulphides. The radiation chemistry literature has example for every amino acid in this case identifying one electron reduction sites

Other amino acids ...

And in this case identifying one electron oxidation sites.

For each amino acid, based on these sites. Models of pathways exist.



The Dream is alive ...

- We have a multitrack model consistent with multiple experimental observations of disulphide damage.
- Good data exist to provide models for other amino acids.
- Metals are a different talk
- With tested models and rate information we have the necessary information to model damage processes.
- We just have to wait for molecular dynamics computing power to catch up!

Summary

- Understanding radical destruction as well as formation is important.
- A multi-track model involving both formation and destruction is valid in explaining X-ray induced disulfide bond damage, observed by UV/Visible, EPR and crystallography over a wide dose range.
- Multi-track considerations offer a key step in a comprehensive model of radiation damage that could potentially help identify when damage is likely to be present, to quantitate it, and provide the ability to recover the native unperturbed structure.

The team

Kristin Sutton – Hauptman-Woodward

William Bernard, Paul Black and Kermit Mercer –
University of Rochester

Robin Owen – Diamond

Elspeth Garman - Oxford

Thank you and questions?



esnell@hwi.buffalo.edu

Gordon Research Seminar on Diffraction Methods in
Structural Biology,
July 26th-27th, Bates College Maine, Grad Students,
Post-Docs dedicated meeting.

Gordon Research Conference on Diffraction Methods in
Structural Biology
July 27th to August 1st, Bates College, Maine:
All welcome

The exciting program includes X-ray free electron applications development, new instruments for diffraction, growing crystals for the next generation, data to maps, maps to models, other scattering methods, industrial perspectives and biology being impacted by these techniques

Details at <https://www.grc.org/programs.aspx?year=2014&program=diffrac>, see Oli Zeldin (vice-chair for the GRS or Eddie Snell (vice chair for the GRC) for more details. Deadline June 29th – meetings have limited places.